

# Influence of Different Atomic Percentage of Silver Doped Nano Zinc Oxide on Titanium Dioxide Seeded Substrate

Siti Zulaikha Umbaidillah<sup>1,2\*</sup>, Nur Amierah M. Asib<sup>1,2</sup>, Nurul Afaah Abdullah<sup>1,2</sup>, Mohamad Rusop<sup>1,3</sup>, Zuraidah Khusaimi<sup>1,2</sup>

<sup>1</sup>Faculty of Applied Sciences, Universiti Teknologi MARA, 40450 Shah Alam, Selangor, Malaysia

<sup>2</sup>Nano-SciTech Centre, Institute of Science, Universiti Teknologi MARA, 40450 Shah Alam, Selangor, Malaysia

<sup>3</sup>Nano-Electronic Centre, Faculty of Electrical Engineering, Universiti Teknologi MARA, 40450 Shah Alam, Selangor, Malaysia

\*Corresponding author E-mail: [zulaikhaumbaidillah95@gmail.com](mailto:zulaikhaumbaidillah95@gmail.com)

## Abstract

Non-doped ZnO/TiO<sub>2</sub> and Silver (Ag) doped ZnO/TiO<sub>2</sub> nanostructures thin film were successfully synthesized on glass substrate by using sol-gel spin coating technique for deposition of TiO<sub>2</sub> seed layer and solution immersion method for growth of Ag-doped ZnO/TiO<sub>2</sub> nanostructure. Different atomic percentage (at%) which is 0.5, 1.0, 1.5, 2.0 and 2.5 at% of Ag doped were added in 0.4 M of Zn<sup>2+</sup> solution. The EDX result revealed that the sample was composed of Zn, O and Ag elements which confirmed the existence of Ag element in the sample. The XRD spectra shows that the intensity of the (002) peak of 0.5 at % Ag-doped ZnO/TiO<sub>2</sub> was the highest compared to other samples and all the samples revealed polycrystalline structure belonging to the ZnO hexagonal wurtzite type. The UV-vis absorbance also indicates that 0.5 at% Ag-doped ZnO/TiO<sub>2</sub> has the highest absorbance and non-doped ZnO/TiO<sub>2</sub> displayed the lowest absorbance compared to the other sample. Thus, 0.5 at% of Ag-doped ZnO/TiO<sub>2</sub> is the best candidate for optical application due to the higher intensity and greater absorbance.

**Keywords:** Ag-doped ZnO/TiO<sub>2</sub>; TiO<sub>2</sub> seed layer; solution immersion method

## 1. Introduction

Zinc oxide (ZnO) is a recognized II-VI semiconducting material with direct band gap energy (3.37 eV) and large exciton binding energy (60 meV) and it has attracted considerable interest in the research community. Although ZnO had been considered for research in the past decades and due to brand new elementary physical properties and applications of nano-device, the renewed interests are focused on the low-dimensional nanostructures, such as nanoparticles, nanorods, nanowires and nanotubes. ZnO also have their own benefits such as inexpensive material, non-toxicity, chemical stability, high transparency in the visible and near infrared spectral region [1]. Due to the physical and optical properties of ZnO, it offers many application in optoelectronic devices such as light emitting diodes (LEDs), UV detectors, and semiconductor laser [2].

TiO<sub>2</sub> is a suitable candidate to introduce to the ZnO matrices as TiO<sub>2</sub> can act as a catalytic promoter during the involved reaction in a chemical process [3]. In order to overcome the interfacial layer mismatch between the substrate and ZnO, TiO<sub>2</sub> is used as a seed layer where it will act as nucleation site and assist the process of epitaxial growth on the seed layer coated glass substrate [4]. It can significantly modify the optical and physical properties of thin film. TiO<sub>2</sub> have also been used in variety of application nowadays due to its' excellent properties such as high chemical stability, good semiconductor properties, and strong oxidized ability [5]. TiO<sub>2</sub> has been used in wide range of application such as chemical sensors, solar cells, for hydrogen gas evolution, as a pigment self-cleaning surfaces and environment purification application [6].

Doped ZnO with an appropriate foreign element will creates the formation of acceptor or donor levels in the forbidden band gap which has the tendency to altering the optical and electrical properties of ZnO [7]. There are various dopant in Group-IB (copper, silver and gold) among possible acceptor dopant that can be doped with ZnO samples and silver (Ag) have been reported as the best candidate to use as a dopant element in ZnO due to its properties which is larger ionic size, high solubility, larger and minimum orbital energy [8]. Ag can also act as the acceptor in ZnO which can be used in the places of substitution and interstitial [9]. According to previous literature [10], the incorporation of Ag in ZnO lattice reduced donor density which indicates that Ag could be an effective acceptor in ZnO.

In the case of sensing properties, ZnO is regarded as one of the most important materials for this device because of its unique characteristics such as high saturation drift velocity, strong radiation hardness, ease of manufacturing and low cost [11]. However, pure ZnO materials typically exhibit a relatively poor sensing performance due to the fast recombination rate of photoexcited electron-hole pairs [12, 13]. In order to handle the issues and improve the sensing properties of ZnO materials, doping processes have been applied to tailor certain properties of ZnO [14, 15]. Many researchers have focussed research efforts to improve the cell efficiency by optical absorption. For example, Ko and Yu [16] synthesized Ag-doped ZnO nanorod arrays and found that Ag incorporation can greatly increase the optical absorption.

In this work, the various atomic percentage (at%) of Ag-doped ZnO have been synthesized by using solution immersion method for the growth of Ag-doped ZnO and spin coating technique for TiO<sub>2</sub> seed layer. The effect of various atomic percentage of Ag-doped ZnO were characterized by XRD, EDX and UV-Vis.

## 2. Experimental

### 2.1. Preparation of Substrate

Substrate which is the glass microscope slide was cut by using a diamond cutter and cleaned ultrasonically by using 3 type of solution which was ethanol, acetone and deionized (DI) water and dried by using argon gas.

### 2.2. Preparation of TiO<sub>2</sub> Seed layer

Titanium (IV) butoxide was used as the starting material for preparation of TiO<sub>2</sub>. Under constant stirring, titanium (IV) butoxide was dissolved in ethanol, glacial acetic acid (to speed up chemical reaction) and Triton-x-100 (helps to decrease the surface tension of the solution). The mixture was heated at 60 °C for 2 hours and allowed to age for 24 hours with continuous stirring. The deposition of seven layers of TiO<sub>2</sub> on the glass substrate were performed by using spin coating technique and followed by drying process at 120 °C. To achieve crystallization, the TiO<sub>2</sub> seed layers were annealed in Pro-Therm furnace, at 450 °C for an hour. **Fig. 1** shows the schematic diagram of spin coating technique.

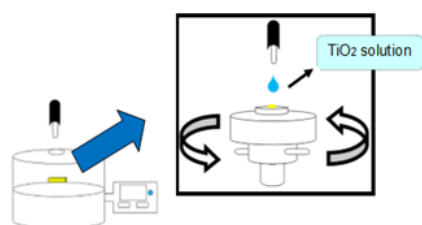


Fig. 1: Schematic diagram of spin coating technique

### 2.3. Preparation of Zn<sup>2+</sup> solution with addition of Ag-doped

0.04 M of zinc nitrate hexahydrate (Zn(NO<sub>3</sub>)<sub>2</sub>·6H<sub>2</sub>O) and hexamethylene tetraamine, (HMTA) (C<sub>6</sub>H<sub>12</sub>N<sub>4</sub>) and silver nitrate (AgNO<sub>3</sub> (0.5at%)) were used to prepare the starting solution. Each compound was prepared by weighing the powder and then dissolved in DI water. These prepared solutions were mixed together and heated at 60 °C for 1 hour and went through aging process for 24 hours with continuous stirring, at room temperature. The preparation of doped Zn<sup>2+</sup> solution with addition of Ag-doped was repeated to other atomic percentage which is 1.0, 1.5, 2.0 and 2.5 at%.

Solution immersion method was used to fabricate Ag-doped ZnO on TiO<sub>2</sub> seed layer. The TiO<sub>2</sub> seed layer thin film substrate was suspended in reaction vessels which contain prepared Zn<sup>2+</sup> solution. The growth of Ag-doped ZnO took place by immersion in water bath for 4 hours at 90 °C. After the deposition process, the substrate was taken out and rinsed with DI water for several times followed by annealing process at 500 °C for 1 hour. **Fig. 2** shows the schematic diagram of solution immersion method.

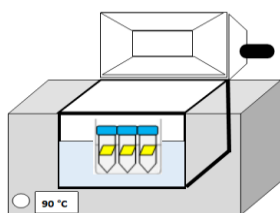


Fig. 2: Schematic diagram of solution immersion method

### 2.4. Characterization of sample

The effect of different atomic percentage of Ag-doped ZnO/TiO<sub>2</sub> to structural was carried out using X-ray diffractometry XRD

(PANalytical X'Pert PRO model, 6000 with CuK $\alpha$  radiation operated at 30 kV and 20 Ma,  $\lambda=1.5406$  Å). The optical analyses of the samples were observed by UV-Vis Spectrophotometer (VARIAN 5000) where the UV-vis absorption spectrum was recorded in the range of 300–800 nm. The EDX analysis (Carl Zeiss Supra 40 VP) was used to confirm the elemental composition of the sample.

## 3. Result and Discussion

### 3.1. X-Ray Diffraction (XRD)

The crystal structure of non-doped ZnO/TiO<sub>2</sub> and Ag-doped ZnO/TiO<sub>2</sub> thin film were explored using measured XRD patterns, as shown in **Fig. 3**. The XRD pattern indicates all films (except peaks showed by star (\*) symbol) revealed polycrystalline with a structure that belongs to the ZnO hexagonal wurtzite type. It shows a distinct peak at 34.42 which corresponds to (002) Miller indices, as well as peaks at 31.77 and 36.25, corresponding to (100) and (101) Miller indices, respectively (JCPDS 00-036-1451). Moreover, the small peak that showed by star symbol (\*) of (101) plane observed at 25.35 is owing to presence of TiO<sub>2</sub> anatase (JCPDS 00-004-0477).

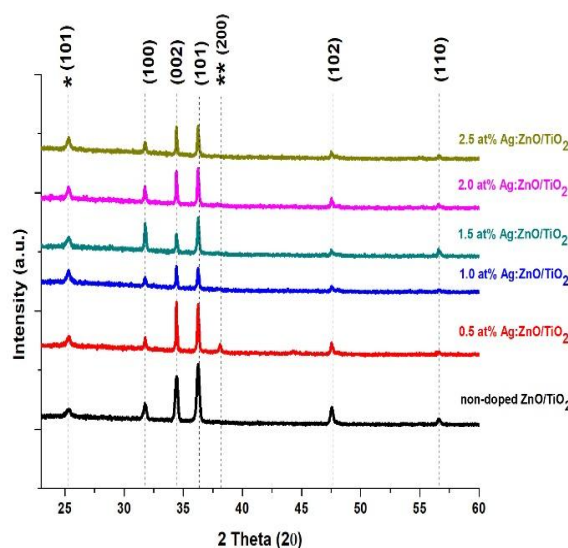


Fig. 3: XRD pattern of non-doped and Ag-doped ZnO/TiO<sub>2</sub>

XRD spectra reveals that the addition diffraction peak shown at 38.06 could be attributed for face cubic structure of metallic Ag (\*\*\*) with space group Pn-3m (No. 224) (JCPDS 00-041-1104) for 0.5at% Ag-doped ZnO nanostructure. Appearance of Ag peaks in the XRD diffraction pattern clearly confirmed the formation of crystalline silver in the ZnO nanorod [17]. However, the absences of Ag peak were observed for Ag doping amounts that higher than 0.5 at%, this is due to the low solubility of Ag in ZnO [18]. High amount of Ag<sup>+</sup> that caused the agglomeration cannot incorporate well in ZnO lattice or interstitial site. Thus, this phenomenon maybe contributes to the absence of Ag peak in XRD pattern. Besides, the result shows that all the ZnO/TiO<sub>2</sub> thin film have (002) Miller indices as preferred orientation. The intensity of the (002) peak at 34.42 of 0.5at% Ag-doped ZnO/TiO<sub>2</sub> has the highest intensity compared to non-doped and the other doped samples, displaying that at 0.5at% of Ag-doped improves the crystallinity of the fabricated ZnO/TiO<sub>2</sub> nanorods. The crystallite size of the non-doped and doped samples were calculated from the Scherrer's formula [19]. **Table 1** shows the crystallite size for non-doped ZnO/TiO<sub>2</sub> and Ag-doped ZnO/TiO<sub>2</sub>

$$D = \frac{0.9 \lambda}{\beta \cos \theta} \quad (1)$$

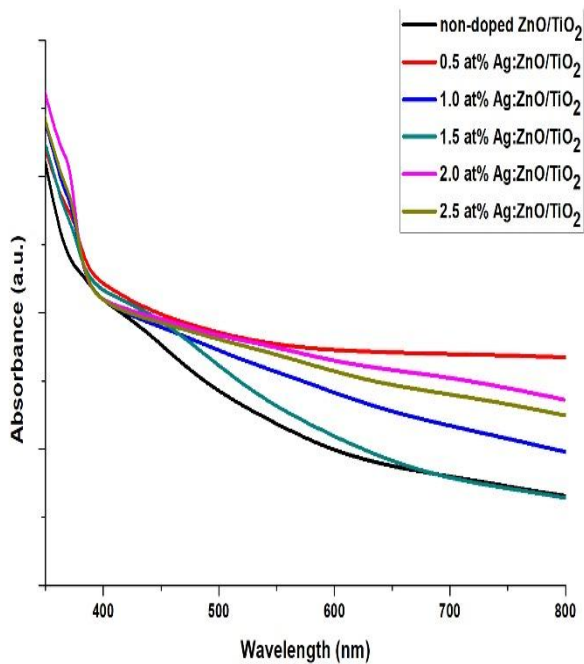
**Table 1:** Crystallite size for non-doped ZnO/TiO<sub>2</sub> and Ag-doped ZnO/TiO<sub>2</sub>.

| Samples                         | Crystallite size (nm) |
|---------------------------------|-----------------------|
| Non-doped ZnO/TiO <sub>2</sub>  | 30.4                  |
| 0.5 at% Ag:ZnO/TiO <sub>2</sub> | 60.4                  |
| 1.0 at% Ag:ZnO/TiO <sub>2</sub> | 58.0                  |
| 1.5 at% Ag:ZnO/TiO <sub>2</sub> | 51.5                  |
| 2.0 at% Ag:ZnO/TiO <sub>2</sub> | 60.7                  |
| 2.5 at% Ag:ZnO/TiO <sub>2</sub> | 63.5                  |

where  $D$  is the crystallite size,  $\lambda$  is the wavelength of Cu  $K\alpha$  (1.5406 Å),  $\beta$  is the peak width at FWHM in radians and  $\theta$  is peak position. The crystallite size at (002) plane is found to be 30.4nm for non-doped ZnO/TiO<sub>2</sub> and for 0.5, 1.0, 1.5, 2.0, 2.5 at% Ag doped ZnO/TiO<sub>2</sub>, the crystallite size was 60.4, 58.0, 51.5, 60.7 and 63.5 nm respectively. The crystallite size is found to increase with Ag dopant. This might be due to the difference ionic radius between Ag<sup>+</sup> ion (0.129nm) and Zn<sup>2+</sup> ion (0.088nm) which lead to segregation of Ag at the region of grain boundary of ZnO [18].

### 3.2. Ultraviolet-Visible Spectrophotometry (UV – Vis)

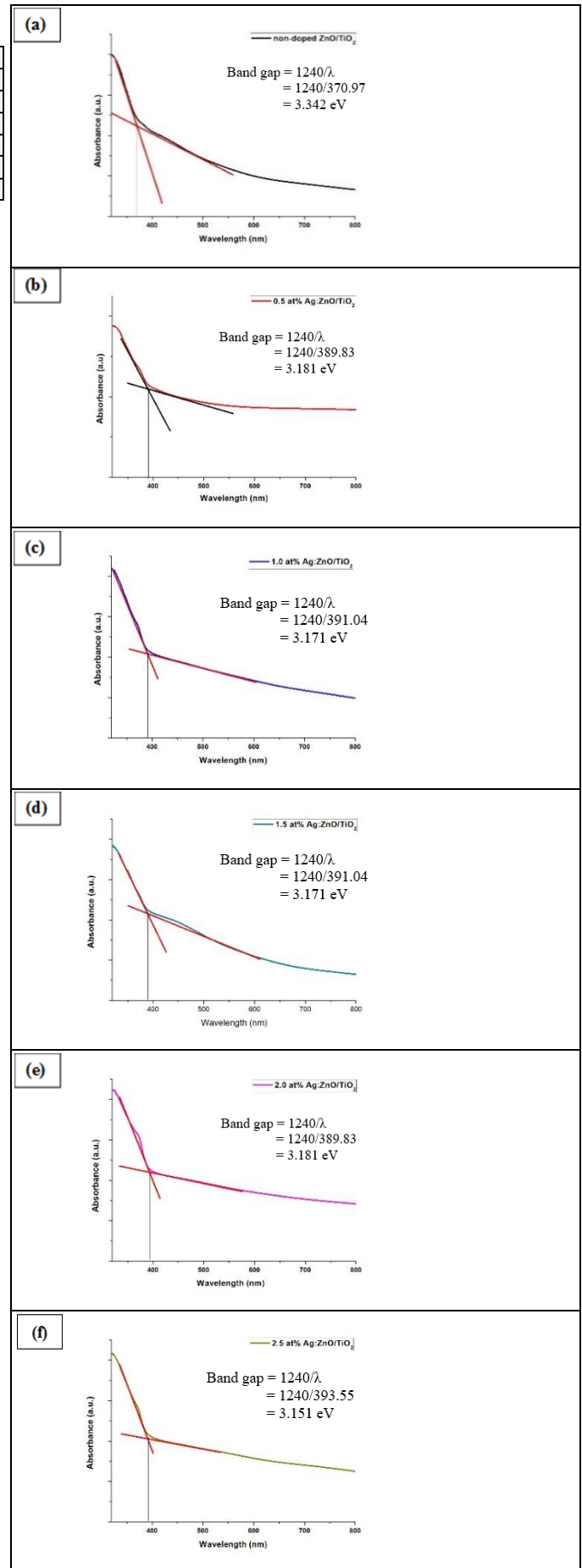
The UV – vis absorbance spectra in the 300 – 800 nm waveband of the synthesis non-doped ZnO/TiO<sub>2</sub> and 0.5, 1.0, 1.5, 2.0 and 2.5 at% doped ZnO/TiO<sub>2</sub> sample are depicted in Fig. 4.

**Fig. 4:** UV-Vis absorption spectra of non-doped and Ag-doped ZnO/TiO<sub>2</sub>

All the samples show strong absorption at 375 nm in UV region and low absorbance value in visible region which indicates the sample has good transparency in visible region. This result displayed that there is no obvious distinctness of absorbance properties between the samples. In this result, Fig.4 shows that 0.5 at% Ag: ZnO/TiO<sub>2</sub> has the highest absorbance and non-doped ZnO/TiO<sub>2</sub> indicates the lowest absorbance compared to the other samples. The strong absorption in the UV region shows that the absorption band of ZnO nanorod was attributed to the intrinsic transition between valence band (VB) and conduction band (CB) [20].

The slope of absorbance spectra is corresponding to the band gap for non-doped and Ag-doped ZnO/TiO<sub>2</sub>. By using energy-wavelength relationship equation [21], the band gap value for each sample has been directly calculated.

$$E = hf = hc/\lambda = 1240 \text{ eV nm} / \lambda \quad (2)$$

**Fig. 5:** UV-Vis absorption spectra of the sample (a) non-doped, (b) 0.5 at% (c) 1.0 at% (d) 1.5 at% (e) 2.0 at% (f) 2.5 at% Ag:ZnO/TiO<sub>2</sub>.

The band gap value for each sample was calculated by using energy-wavelength relationship  $E=hc/\lambda$ . In this relation, E is energy, h is Planck's constant which is  $6.62606957 \times 10^{-34}$  J.s, f is frequency, c is velocity of light which is  $2.99792458 \times 10^8$  m/s and  $\lambda$  is the value of incident wavelength which found from cross link at the edge slope of absorbance spectra as shown in **Fig.5** and the energy band gap of the samples according to the edge of absorbance were tabulated in **Table 2**.

**Table 2:** Energy band gap of the samples according to the edge of absorbance.

| Samples                         | Edge of Absorbance (nm) | Energy band gap (eV) |
|---------------------------------|-------------------------|----------------------|
| Non-doped ZnO/TiO <sub>2</sub>  | 370                     | 3.342                |
| 0.5 at% Ag:ZnO/TiO <sub>2</sub> | 389                     | 3.181                |
| 1.0 at% Ag:ZnO/TiO <sub>2</sub> | 391                     | 3.171                |
| 1.5 at% Ag:ZnO/TiO <sub>2</sub> | 391                     | 3.171                |
| 2.0 at% Ag:ZnO/TiO <sub>2</sub> | 389                     | 3.181                |
| 2.5 at% Ag:ZnO/TiO <sub>2</sub> | 393                     | 3.151                |

Optical energy band gap for Ag-doped ZnO/TiO<sub>2</sub> are 3.181, 3.171, 3.171, 3.181 and 3.151 eV which smaller than the energy band gap of non-doped ZnO/TiO<sub>2</sub>. Decreasing in the energy band gap is may be due to the existence of p-type conductivity in the Ag-doped ZnO/TiO<sub>2</sub> [22]. Formation of p-type in the substance is may be due to the impurity band in energy gap that provided by Ag doping in ZnO/ TiO<sub>2</sub> [22]. The reduction of energy band gap of the samples led to improve the proficiency in the use of these material in optoelectronic devices [23].

### 3.3. Energy Dispersive X-ray (EDX)

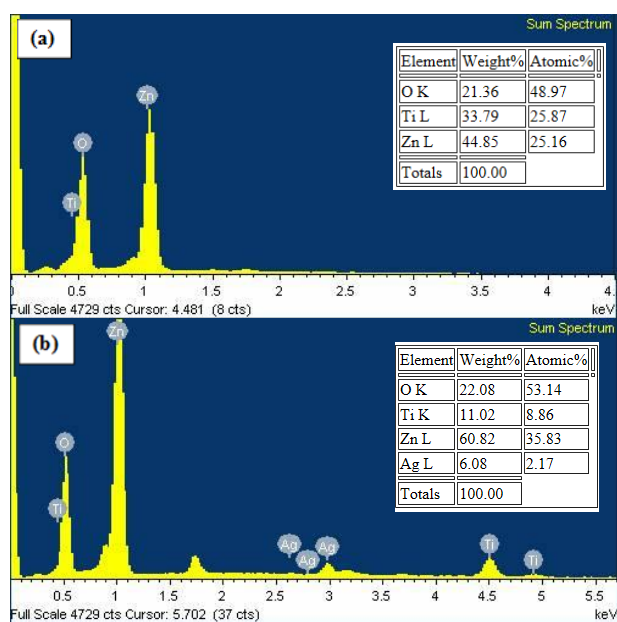


**Fig.6:** EDX spectra of the (a) non-doped ZnO/TiO<sub>2</sub> and (b) Ag-doped ZnO/TiO<sub>2</sub>

In order to investigate the elemental composition of the sample, EDX analysis was used. The elemental composition of non-doped and Ag-doped ZnO/TiO<sub>2</sub> sample confirmed the present of ZnO, Ti and O element as shown in **Fig.6**. EDX spectrum of Ag-doped ZnO/TiO<sub>2</sub> clearly reveals the existence of Ag element (~2.17 at%) in the sample.

## 4. Conclusion

Non-doped ZnO/TiO<sub>2</sub> and 0.5, 1.0, 1.5, 2.0, 2.5 at% Ag-doped ZnO/TiO<sub>2</sub> were successfully characterized by using XRD, EDX and UV Vis. The crystallite size of Ag-doped samples was larger than non-doped sample and increase in Ag content does not

change the wurtzite hexagonal structure of ZnO. As the concentration of Ag content were varied, the growth of 0.5 at% of Ag-doped ZnO/TiO<sub>2</sub> shows a very good potential to produce a good optical property due to the high absorption in UV region.

## Acknowledgement

We would like to express our gratitude to Ministry of Education Malaysia, Research Management Institute and Universiti Teknologi MARA (UiTM), Shah Alam, Selangor, Malaysia for financial support.

## References

- [1] R. Chander and A. Raychaudhuri, "Electrodeposition of aligned arrays of ZnO nanorods in aqueous solution," *Solid State Communications*, vol. 145, pp. 81-85, 2008.
- [2] J. Hassan, M. Mahdi, A. Ramizy, H. A. Hassan, and Z. Hassan, "Fabrication and characterization of ZnO nanorods/p-6H-SiC heterojunction LED by microwave-assisted chemical bath deposition," *Superlattices and Microstructures*, vol. 53, pp. 31-38, 2013.
- [3] D. Barreca, E. Comini, A. P. Ferrucci, A. Gasparotto, C. Maccato, C. Maragno, *et al.*, "First example of ZnO-TiO<sub>2</sub> nanocomposites by chemical vapor deposition: structure, morphology, composition, and gas sensing performances," *Chemistry of Materials*, vol. 19, pp. 5642-5649, 2007.
- [4] N. A. M. Asib, A. N. Afaah, A. Aadila, M. R. Mahmud, Y. C. Lim, S. A. H. Alrokayan, *et al.*, "Effect of molarity of TiO<sub>2</sub> seeded-template to the growth of ZnO nanostructures," *IOP Conference Series: Materials Science and Engineering*, vol. 83, p. 012006, 2015.
- [5] M. Asiah, M. Mamat, Z. Khusaimi, M. Achoi, S. Abdullah, and M. Rusop, "Thermal stability and phase transformation of TiO<sub>2</sub> nanowires at various temperatures," *Microelectronic Engineering*, vol. 108, pp. 134-137, 2013.
- [6] M. R. Hoffmann, S. T. Martin, W. Choi, and D. W. Bahnemann, "Environmental applications of semiconductor photocatalysis," *Chemical reviews*, vol. 95, pp. 69-96, 1995.
- [7] A. Rajan, H. K. Yadav, V. Gupta, and M. Tomar, "Sol-gel derived Ag-doped ZnO thin film for UV photodetector with enhanced response," *Journal of materials science*, vol. 48, pp. 7994-8002, 2013.
- [8] Y. Yan, M. Al-Jassim, and S.-H. Wei, "Doping of ZnO by group-IB elements," *Applied physics letters*, vol. 89, p. 181912, 2006.
- [9] O. Lupan, L. Chow, L. K. Ono, B. R. Cuenya, G. Chai, H. Khallaf, *et al.*, "Synthesis and characterization of Ag-or Sb-doped ZnO nanorods by a facile hydrothermal route," *The Journal of Physical Chemistry C*, vol. 114, pp. 12401-12408, 2010.
- [10] J. Fan and R. Freer, "The roles played by Ag and Al dopants in controlling the electrical properties of ZnO varistors," *Journal of Applied Physics*, vol. 77, pp. 4795-4800, 1995.
- [11] W. Dai, X. Pan, C. Chen, S. Chen, W. Chen, H. Zhang, *et al.*, "Enhanced UV detection performance using a Cu-doped ZnO nanorod array film," *RSC Advances*, vol. 4, p. 31969, 2014.
- [12] L. Hu, L. Zhu, H. He, Y. Guo, G. Pan, J. Jiang, *et al.*, "Colloidal chemically fabricated ZnO: Cu-based photodetector with extended UV-visible detection waveband," *Nanoscale*, vol. 5, pp. 9577-9581, 2013.
- [13] T. Wang, Z. Jiao, T. Chen, Y. Li, W. Ren, S. Lin, *et al.*, "Vertically aligned ZnO nanowire arrays tip-grafted with silver nanoparticles for photoelectrochemical applications," *Nanoscale*, vol. 5, pp. 7552-7557, 2013.
- [14] C.-L. Hsu, Y.-D. Gao, Y.-S. Chen, and T.-J. Hsueh, "Vertical p-type Cu-doped ZnO/n-type ZnO homojunction nanowire-based ultraviolet photodetector by the furnace system with hotwire assistance," *ACS applied materials & interfaces*, vol. 6, pp. 4277-4285, 2014.
- [15] C.-L. Hsu, K.-C. Chen, T.-Y. Tsai, and T.-J. Hsueh, "Fabrication of gas sensor based on p-type ZnO nanoparticles and n-type ZnO nanowires," *Sensors and Actuators B: Chemical*, vol. 182, pp. 190-196, 2013.
- [16] Y. H. Ko and J. S. Yu, "Optical absorption enhancement of embedded Ag nanoparticles with ZnO nanorod arrays," *physica status solidi (a)*, vol. 208, pp. 2778-2782, 2011.

- [17] R. Zamiri, A. Rebelo, G. Zamiri, A. Adnani, A. Kuashal, M. S. Belsley, *et al.*, "Far-infrared optical constants of ZnO and ZnO/Ag nanostructures," *RSC Advances*, vol. 4, pp. 20902-20908, 2014.
- [18] M. Dehimi, T. Touam, A. Chelouche, F. Boudjouan, D. Djouadi, J. Solard, *et al.*, "Effects of Low Ag Doping on Physical and Optical Waveguide Properties of Highly Oriented Sol-Gel ZnO Thin Films," *Advances in Condensed Matter Physics*, vol. 2015, pp. 1-10, 2015.
- [19] M. Marikkannan, V. Vishnukanthan, A. Vijayshankar, J. Mayandi, and J. M. Pearce, "A novel synthesis of tin oxide thin films by the sol-gel process for optoelectronic applications," *Aip Advances*, vol. 5, p. 027122, 2015.
- [20] M. Haase, H. Weller, and A. Henglein, "Photochemistry and radiation chemistry of colloidal semiconductors. 23. Electron storage on zinc oxide particles and size quantization," *The Journal of Physical Chemistry*, vol. 92, pp. 482-487, 1988.
- [21] A. Elaziouti, N. Laouedj, A. Bekka, and R.-N. Vannier, "Preparation and characterization of p-n heterojunction CuBi<sub>2</sub>O<sub>4</sub>/CeO<sub>2</sub> and its photocatalytic activities under UVA light irradiation," *Journal of King Saud University-Science*, vol. 27, pp. 120-135, 2015.
- [22] S. Hosseini, I. A. Sarsari, P. Kameli, and H. Salamati, "Effect of Ag doping on structural, optical, and photocatalytic properties of ZnO nanoparticles," *Journal of Alloys and Compounds*, vol. 640, pp. 408-415, 2015.
- [23] M. K. Gupta, N. Sinha, and B. Kumar, "p-type K-doped ZnO nanorods for optoelectronic applications," *Journal of Applied Physics*, vol. 109, p. 083532, 2011.